Scaling of elliptic flow, recombination, and sequential freeze-out of hadrons in heavy-ion collisions

Min He,[1] Rainer J. Fries,[1,2] and Ralf Rapp[1]

[1]*Cyclotron Institute and Department of Physics and Astronomy, Texas A&M University, College Station, Texas 77843, USA*

[2]*RIKEN/BNL Research Center, Brookhaven National Laboratory, Upton, New York 11973, USA*

(Received 9 June 2010; revised manuscript received 31 August 2010; published 21 September 2010)

The scaling properties of elliptic flow of hadrons produced in ultrarelativistic heavy-ion collisions are investigated at low transverse momenta, $p_T \lesssim 2$ GeV. Utilizing empirical parametrizations of a thermalized fireball with collective-flow fields, the resonance recombination model (RRM) is employed to describe hadronization via quark coalescence at the hadronization transition. We reconfirm that RRM converts equilibrium quark distribution functions into equilibrated hadron spectra including the effects of space-momentum correlations on elliptic flow. This provides the basis for a controlled extraction of quark distributions of the bulk matter at hadronization from spectra of multistrange hadrons which are beligeved to decouple close to the critical temperature. The resulting elliptic flow from empirical fits at the BNL Relativistic Heavy Ion Collider exhibits transverse kinetic-energy and valence-quark scaling. Utilizing the well-established concept of sequential freeze-out, the scaling at low momenta extends to bulk hadrons (π, K, p) at thermal freeze-out, albeit with different source parameters compared to chemical freeze-out. Elliptic-flow scaling is thus compatible with both equilibrium hydrodynamics and quark recombination.

DOI: 10.1103/PhysRevC.82.034907 PACS number(s): 25.75.−q, 12.38.Mh, 14.40.Lb

I. INTRODUCTION

Ultrarelativistic heavy-ion collisions (URHICs) enable the creation and study of superdense, strongly interacting matter, possibly associated with the formation of novel phases where partons deconfine and chiral symmetry is restored [1]. One major finding by the experimental program at the Relativistic Heavy Ion Collider (RHIC) at Brookhaven National Laboratory is the large azimuthal anisotropy of hadron transverse-momentum (p_T) spectra in noncentral nuclear collisions, the so-called elliptic flow [2]. It is quantified by the second harmonic coefficient $v_2(p_T)$ in the Fourier expansion of the azimuthal angle ϕ for the p_T spectra of hadrons.

Experimental measurements suggest that the behavior of $v_2(p_T)$ may be classified into three regimes. At high transverse momentum, $p_T \gtrsim 6$ GeV, the azimuthal anisotropy is believed to be due to the path-length dependence of high-energy partons as they traverse the hot medium and lose energy. We will not be concerned any further with this mechanism in the present work. At low transverse momentum, $p_T \lesssim 2$ GeV, v_2 increases with p_T essentially linearly but with a delayed onset for hadrons with increasing mass, giving rise to the so-called mass ordering of elliptic flow [3]. This regime is well described by hydrodynamic simulations and thus indicates a large degree of equilibration, encompassing more than 90% of the observed particles [4–8]. At intermediate transverse momenta, $2 \lesssim p_T \lesssim 6$ GeV, $v_2(p_T)$ saturates and exhibits a remarkable scaling between baryons and mesons [9],

$$v_2(p_T) = n_q v_2^{(q)}(p_T/n_q)\,, \tag{1}$$

where n_q denotes the number of valence quarks contained in hadron h. Equation (1), also known as constituent-quark number scaling (CQNS), has been successfully described in the framework of quark coalescence models, where quarks recombine into hadrons at the transition from partonic to hadronic matter [10]. In line with Eq. (1), these models thus imply that the observed hadron elliptic flow can be reduced to a universal quark elliptic flow at hadronization. This assertion, however, requires several simplifying assumptions. First, interactions in the subsequent hadronic evolution (between hadronization at $T_c \simeq 180$ MeV and kinetic freeze-out at $T_{\rm fo} \simeq 100$ MeV) are neglected. Furthermore, Eq. (1) can only be derived in instantaneous quark coalescence models where energy conservation is violated and narrow hadron wave functions in momentum space are utilized. In addition, the underlying quark distribution functions are assumed to factorize in coordinate and momentum space, implying that the elliptic flow of the system is implemented point-by-point (i.e., locally), rather than through a space-dependent flow field which is a consequence of a collectively expanding source. The implementation of realistic space-momentum correlations into quark coalescence models has indeed been proved difficult [11]. Finally, quark coalescence models typically do not comply with the principle of detailed balance, implying that the proper equilibrium limit cannot be established. This hampers attempts to extend the description into the low-p_T regime where thermalization is believed to prevail. This became a more pressing issue once it was realized that CQNS can be generalized to encompass both low and intermediate p_T if v_2 is plotted versus transverse kinetic energy, $\mathrm{KE}_T \equiv m_T - m$, where $m_T = (p_T^2 + m^2)^{1/2}$ is the hadron's transverse mass [12–17]. In this representation, elliptic-flow data for all observed hadrons fall onto one universal curve for v_2/n_q versus KE_T/n_q [12,13].

Progress on the above issues has been recently reported by reformulating the quark coalescence process at hadronization in terms of resonant $q\bar{q} \to M$ scattering (M: meson) [18,19]. Implementing the underlying cross section into a Boltzmann transport equation (e.g., in the Breit-Wigner approximation) not only guarantees energy-momentum conservation but also

satisfies detailed balance and thus leads to the correct thermal-equilibrium limit. It has been verified [18] that the meson spectra resulting from the resonance recombination model (RRM) are compatible with CQNS, Eq. (1), in the factorized (local) approximation to $v_2(p_T)$. A further step has been taken in Ref. [20] where the RRM has been applied to more realistic quark distribution functions as generated by relativistic Langevin simulations within an expanding QGP fireball [21] for semicentral Au-Au collisions at RHIC. Since the Brownian-motion approximation underlying the Langevin process is only reliable for relatively massive and/or high-momentum particles, $m_T \gg T$, the results have been restricted to charm and strange quarks. Under inclusion of the full space-momentum correlations imprinted on the quark distributions by the hydrodynamiclike flow fields of the expanding fireball, the elliptic flow of ϕ and J/ψ mesons was found to exhibit CQNS in KE_T from 0 to $\sim$3 GeV, which encompasses both low and intermediate p_T, i.e., the quasithermal and kinetic regimes. However, several important questions remain, e.g., the manifestation of CQNS and KE_T scaling for bulk (light) particles in the low-p_T (thermal) regime, the robustness and generality of the flow fields utilized in the fireball simulations or the role of reinteractions in the hadronic phase. A thorough understanding of these issues, in connection with a quantitative description of hadron data, is hoped to ultimately enable the extraction of quark distribution functions just prior to the conversion to hadronic degrees of freedom, and thus to quantitatively establish the presence of a collectively expanding partonic source in URHICs.

In the present paper, we investigate the scaling properties of hadron spectra by focusing on the low-p_T regime coupled with the assumption of complete kinetic equilibration. We will utilize the RRM to convert locally equilibrated quark distribution functions into hadron spectra using a blast-wave-type quark source with realistic flow fields at the hadronization transition (including space-momentum correlations characteristic of hydrodynamic simulations). Contrary to earlier work [20], we do not attempt to generate the flow fields from a dynamic evolution, but rather extract them from empirical fits to hadron p_T spectra and elliptic flow. In fact, after verifying that resonance recombination converts collective, locally equilibrated quark distribution functions into equilibrium hadron distributions with identical (space-momentum-dependent) collective properties, one can adopt the source parametrization at the hadron level and thus readily extend the description to baryons. For this part of the investigation, we focus on multistrange hadrons (i.e., hadrons containing at least two strange and/or antistrange quarks) which are believed to kinetically decouple close to the hadronization transition. This notion is supported by empirical blast-wave fits to RHIC and SPS data [1,22,23], as well as by the putative absence of resonances that these hadrons could form in interactions with bulk particles such as pions, kaons or nucleons (hadronic resonances drive the collective expansion of the hadronic phases in URHICs). We refer to hadrons decoupling close to $T_c \simeq 180$ MeV as "group-I" particles, which are thus the prime candidates to infer properties of the quark phase just above the critical temperature. A description of KE_T scaling in the low-p_T regime is incomplete without the bulk hadrons π, K and p. These are well-known to interact quasielastically via resonance formation, resulting in a kinetic freeze-out at lower temperature, $T_{\mathrm{fo}} \simeq 100$ MeV. We refer to these as "group-II" particles and introducing a second source parametrization by fitting their spectra and v_2 with a space-dependent elliptic flow field at T_{fo}. We then investigate the robustness of the empirical scaling by interchanging the sources for group-I and group-II particles. We also reevaluate the question of resonance feed-down contributions to the pion v_2 for which differing results exist in previous works.

Our article is organized as follows. In Sec. II we recall basic features of resonance recombination, specifically its equilibrium limit in the presence of anisotropic flow fields. In Sec. III we quantitatively construct realistic flow fields for semi-central Au-Au collisions at RHIC using group-I particle freeze-out close to the hadronization transition. In Sec. IV we investigate KE_T and n_q scaling for group-I and bulk particles in a sequential freeze-out picture and evaluate its stability. We summarize and conclude in Sec. V.

II. RESONANCE RECOMBINATION MODEL AND EQUILIBRIUM LIMIT

Early quark coalescence models which employed instantaneous approximations in the recombination of quarks [10,24] were quite successful in providing an explanation for two rather unexpected phenomena in hadron spectra at intermediate p_T in Au-Au collisions at RHIC. Specifically, these were the enhancement of baryon-to-meson ratios ($B/M = p/\pi$, Λ/K) over their values measured in p-p collisions, as well as CQNS of $v_2(p_T)$. While an enhanced B/M ratio is also a natural outcome of hydrodynamic flow, the latter is not expected to generate enough yield to dominate hadron production at $p_T > 2$–3 GeV. The instantaneous projection of parton states onto hadron states conserves three-momentum by construction, but energy conservation is violated due to the sudden approximation [11]. This approximation is believed to be viable at intermediate p_T where corrections are expected to be of order $O(Q/p_T)$ with $Q = m - m_q - m_{\bar{q}}$ (m: meson mass, $m_{\bar{q},q}$: antiquark/quark mass), albeit with unknown coefficient [18]. However, this poses a significant problem at low p_T and/or for hadrons (resonances) with large binding energy (Q value).

In Ref. [18], quark coalescence in an interacting medium in the vicinity of the hadronization transition was reinterpreted as a process akin to the formation of resonances, $q + \bar{q} \rightleftharpoons M$, and implemented via a Boltzmann equation

$$p^\mu \partial_\mu f_M(t, \vec{x}, \vec{p}) = -m\Gamma f_M(t, \vec{x}, \vec{p}) + p^0 \beta(\vec{x}, \vec{p}), \qquad (2)$$

where $f_M(t, \vec{x}, \vec{p})$ denotes the phase-space density of the meson, and the gain term is given by

$$\beta(\vec{x}, \vec{p}) = \int \frac{d^3p_1 d^3p_2}{(2\pi)^6} f_q(\vec{x}, \vec{p}_1) f_{\bar{q}}(\vec{x}, \vec{p}_2) \times \sigma(s) v_{\mathrm{rel}}(\vec{p}_1, \vec{p}_2) \delta^3(\vec{p} - \vec{p}_1 - \vec{p}_2)\,. \qquad (3)$$

The use of an explicit (resonant) cross section automatically satisfies energy-momentum conservation. For simplicity it has been modeled by a relativistic Breit-Wigner form,

$$\sigma(s) = g_\sigma \frac{4\pi}{k^2} \frac{(\Gamma m)^2}{(s-m^2)+(\Gamma m)^2}, \tag{4}$$

where the same reaction rate Γ is used as in the loss term, the first term on the right-hand side of Eq. (2), and g_σ is the degeneracy factor. This guarantees detailed balance, which is essential for recovering thermodynamic equilibrium in the long-time limit, $\Delta\tau \gg 1/\Gamma$. If hadronization is rapid enough to produce hadrons in equilibrium, as it seems to be the case for the bulk of hadrons in URHICs, this limit is applicable, and the resulting hadron-momentum distribution is given by

$$f_M^{\rm eq}(\vec{p}) = \frac{E_M(\vec{p})}{m\Gamma} \int d^3x \beta(\vec{x}, \vec{p}). \tag{5}$$

For more details, we refer the reader to Ref. [18]. It is well known that the unique equilibrium solution of a Boltzmann transport equation is a Boltzmann distribution if and only if energy conservation as well as detailed balance are satisfied. The RRM complies with these requirements. In the remainder of this section, we will verify numerically that Eq. (5) recovers the thermal Boltzmann distribution for mesons in the presence of a spatially dependent anisotropic flow field at the quark level (in previous work [18,20], this has only been exemplified for p_T spectra, not for v_2).

As a first test, we study ϕ mesons in an azimuthally symmetric and longitudinally boost-invariant fireball. The phase-space densities of the input strange and antistrange quarks ($m_s = 0.45$ GeV) are parametrized through a blast wave with radial flow velocity $\vec{v}(\vec{r}) = v_0 \cdot \vec{r}/R_0$. We compare the result for ϕ mesons ($m_\phi = 1.02$ GeV, $\Gamma_\phi = 0.05$ GeV) calculated from resonance recombination of s and $\bar{s}$, Eq. (5), with the direct blast-wave expression for the ϕ meson with identical flow field and temperature as for the quark input. Figure 1 shows that both ways of computing the ϕ spectra are

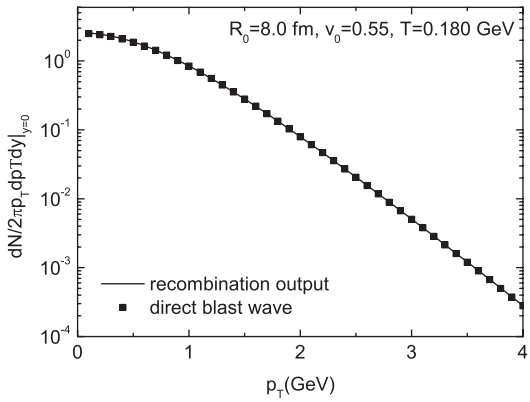

FIG. 1. Comparison of ϕ-meson p_T spectra computed from (i) resonance recombination of strange quarks using blast-wave flow fields for strange quarks (rectangles), and (ii) a direct application of an equilibrium blast-wave distribution (solid line) with the same flow field as for quarks (solid line). The hadronization temperature has been chosen at $T_c = 180$ MeV and the radial flow at the surface as $v_0 = 0.55$.

in excellent agreement. We have reconfirmed that the results are insensitive to variations of the resonance width Γ when ensuring $\Gamma \lesssim Q$ with $Q = m_\phi - (m_s + m_{\bar{s}})$ [18].

To account for anisotropic flow fields which are suitable for generating configurations reminiscent of hydrodynamic simulations for fireballs in noncentral (azimuthally asymmetric) nuclear collisions, we adopt in this work the parametrization introduced by Retière and Lisa (RL) [25]. It assumes longitudinal boost invariance [26] and parametrizes the transverse flow rapidity as a function of radius r and spatial azimuthal angle ϕ_s as

$$\rho(r, \phi_s) = \widetilde{r}\,[\rho_0 + \rho_2 \cos(2\phi_b)]\,, \tag{6}$$

where ρ_0 represents the average radial flow rapidity and ρ_2 the anisotropy of transverse flow. The angle ϕ_b of the flow vector is generally tilted from the position angle ϕ_s (both angles are measured with respect to the reaction plane) which can be reflected by the relation

$$\tan\phi_b = \left(\frac{R_{\rm x}}{R_{\rm y}}\right)^2 \tan\phi_s\,. \tag{7}$$

This ansatz is motivated by the picture that the transverse boost is locally perpendicular to elliptical subshells [25]. The transverse flow rapidity $\rho(r, \phi_s)$ is assumed to increase linearly with the normalized "elliptic radius", defined as

$$\widetilde{r} = \sqrt{r^2\cos^2\phi_s/R_{\rm x}^2 + r^2\sin^2\phi_s/R_{\rm y}^2}\,. \tag{8}$$

We emphasize that this flow field incorporates space-momentum correlations that are considered a much more realistic representation of a collectively expanding source than the factorized ansatz of a "local" v_2 (independent of position) as often adopted in quark coalescence model calculations.

Using the RL parametrization, the differential momentum spectrum for a particle i directly emitted from the source takes the form [5,25,27]

$$\frac{dN_i}{p_T\,dp_T\,d\phi_p\,dy} = \frac{2g_i}{(2\pi)^3}\tau_f\, m_T\, e^{\mu_i/T_f} \times \int r\,dr \int d\phi_s\, K_1(m_T, T, \beta_T)\, e^{\alpha_T \cos(\phi_p - \phi_b)}, \tag{9}$$

where T_f is the freeze-out temperature at constant longitudinal proper time τ_f, μ_i the chemical potential of particle i, g_i the spin-isospin degeneracy factor, K_1 a modified Bessel function, and $\alpha_T = p_T/T_f \sinh\rho(r, \phi_s)$, $\beta_T = m_T/T_f \cosh\rho(r, \phi_s)$. Equation (9) has been written in the Boltzmann approximation, which works well for sufficiently heavy particles; we will, however, use Bose distributions for pions. From Eq. (9) we can calculate the elliptic flow of particle i as

$$v_2^i(p_T) = \frac{\int_0^{2\pi} d\phi_p \cos(2\phi_p) \frac{dN_i}{p_T\,dp_T\,d\phi_p\,dy}}{\int_0^{2\pi} d\phi_p \frac{dN_i}{p_T\,dp_T\,d\phi_p\,dy}}\,. \tag{10}$$

With the RL parametrization for an anisotropic flow field, we are now in position to compare the elliptic flow generated

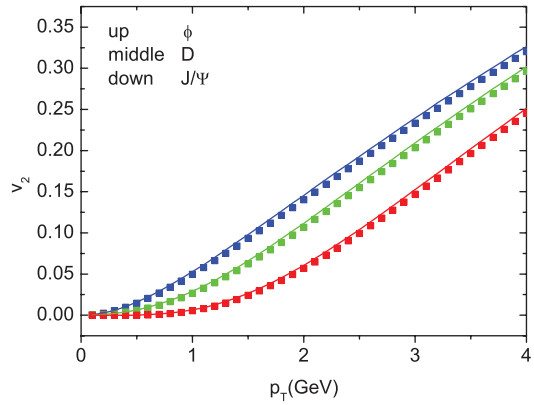

FIG. 2. (Color online) Comparison of elliptic flow for ϕ, D, and J/ψ mesons (top to bottom) computed from (i) resonance recombination of strange quarks (symbols) and (ii) a direct application of the blast-wave expression at the meson level (lines). Both quark and meson distributions are based on the same anisotropic flow field constructed from the RL parametrization with $T_c = 180$ MeV, $R_x = 7.5$ fm, $R_y = 8.5$ fm, $\rho_0 = 0.66$, and $\rho_2 = 0.07$.

for coalesced mesons in the RRM for locally equilibrated quark distributions [Eq. (5)] with the one directly obtained from applying the blast-wave expression (9) at the meson level. We fix the parameters as quoted in the caption of Fig. 2, noting that at this point our aim is not to fit experimental data but to scrutinize generic properties of the RRM. We emphasize again the nontrivial spatial dependence of the flow field figuring into the quark distributions in Eq. (5). To extend the scope of our comparison we also consider, in addition to ϕ mesons, D ($m_D = 1.9$ GeV, $\Gamma_D = 0.1$ GeV) and J/ψ mesons ($m_{J/\psi} = 3.1$ GeV, $\Gamma_{J/\psi} = 0.1$ GeV), as bound states of charm ($m_c = 1.5$ GeV) and light quarks ($m_{u,d} = 0.3$ GeV) and of charm and anticharm quarks, respectively. Figure 2 illustrates the comparison of the meson-$v_2(p_T)$ for RRM and their direct blast-wave counterparts, showing again excellent agreement within numerical accuracy. It is quite remarkable that RRM generates negative v_2 at low p_T for the J/ψ starting from strictly positive $v_2(p_t)$ for the underlying charm-quark distributions. A possibly negative v_2 is a well-known mass effect caused by the depletion of the heavy-particle yield at low momenta in the presence of sufficiently large collective flow [7]. However, we are not aware of any quark coalescence model calculation that has reproduced this result. It demonstrates that the meson distributions resulting from RRM have reached local equilibrium and follow the collective flow of the source. We have checked that the negative v_2 is rather robust against variations of blast-wave parameters. By increasing ρ_0 or ρ_2, the negative value can be amplified.

Combining the results from Figs. 1 and 2, we conclude that hadron phase-space distributions obtained from resonance recombination precisely reflect the collective properties of a source in local equilibrium, explicitly documenting the fact that the RRM achieves this through energy conservation and detailed balance. These insights also imply that the intermediate-p_T regime, where v_2 saturates and shows an explicit dependence on quark number, cannot be in full equilibrium.

III. RECOMBINATION AND QUARK DISTRIBUTIONS AT HADRONIZATION

Based on the verification that resonance recombination maps the collective local-equilibrium properties of the quark source into hadron spectra, we can reverse the strategy and use this as a tool to extract quark distributions by a quantitative study of experimental data on hadrons which arise from quark coalescence. The generality of this argument even allows us to extend the analysis to baryons without having to explicitly calculate their spectra in RRM (which would be more involved than for mesons, since it requires us to recombine three quarks). As alluded to in the Introduction, this procedure can only give access to quark distributions if the subsequent hadronic phase exerts a negligible distortion of the hadron spectra right after their formation around T_c. We label such hadrons as belonging to "group I", and identify multistrange hadrons (ϕ, Ξ, Ω) as the prime candidates currently available from experiment. These hadrons have no well-established resonance excitations on the most abundant bulk particles (π, K, and N) in the hadronic medium, while elastic t-channel exchange processes are suppressed by the Okubo-Zweig-Iizuka (OZI) rule. One can therefore expect that multistrange hadrons do not suffer significant rescattering in the hadronic phase, which is indeed supported by blast-wave fits to experimental data favoring kinetic decoupling not far from T_c. The flow fields extracted for group-I hadrons therefore reflect the collective properties of the quark phase.

We first determine the flow parameters in the RL parametrization by performing a blast-wave fit to the transverse-momentum spectra and elliptic flow of group-I hadrons to experimental data from the solenoidal tracker at RHIC (STAR) detector in midcentral (20–40%) Au-Au collisions. For definiteness (and easier comparison to the RRM calculations in Ref. [20]), we fix the temperature to $T_c = 180$ MeV; we do not utilize it as a parameter but obtain fits of satisfactory quality with this value. The transverse-flow rapidity ρ_0 is mostly governed by fits to the p_T spectra of ϕ, Ξ, and Ω hadrons, while the flow-asymmetry parameter ρ_2 and the fireball's spatial eccentricity R_y/R_x are driven by fitting the elliptic flow of Ξ and ϕ. The resulting RL blast-wave curves are shown with data in Fig. 3, and the central values of the parameters are collected in Table I. As to be expected, the slopes of the spectra can be fitted well. The absolute normalizations are also reproduced reasonably well, which is confirmed by the Ω/ϕ ratio shown on a linear scale in the lower panel of Fig. 3. Degeneracy factors for spin and isospin are taken into account, but baryon chemical potential and the strangeness suppression factor γ_s are neglected in

TABLE I. Parameter values for kinetic freeze-out temperature T_f in MeV, radial-flow rapidity ρ_0, rapidity asymmetry ρ_2, and elliptic radii R_x and R_y in fm, for group-I and -II hadrons using the RL blast-wave expression for midcentral Au-Au collisions at RHIC.

Group	T_f	ρ_0	ρ_2	R_x	R_y
I	180	0.75	0.072	7.5	8.9
II	110	0.93	0.055	11.0	12.4

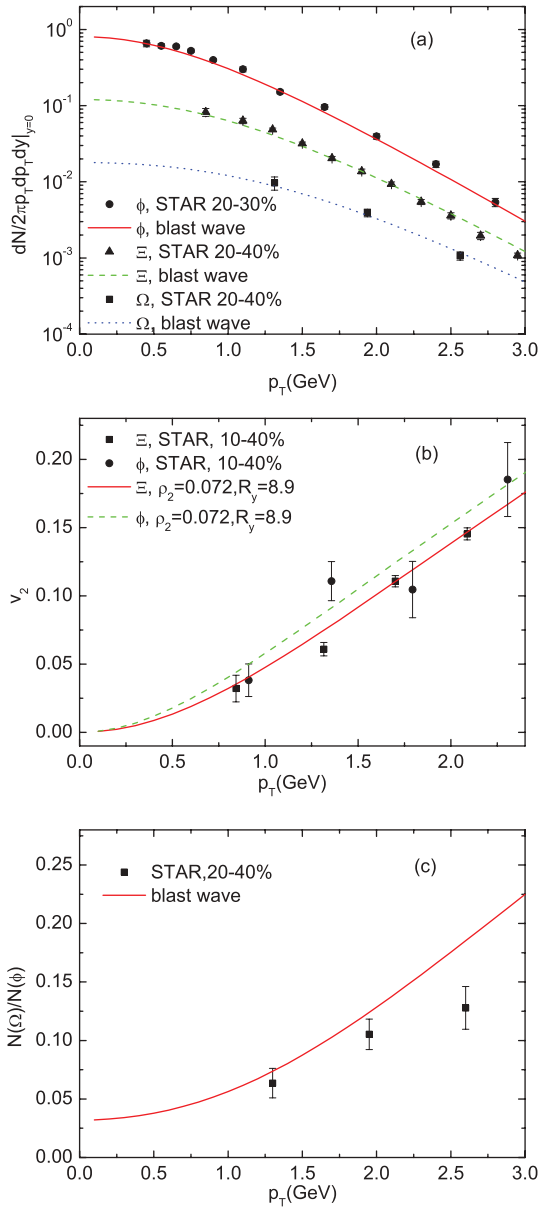

FIG. 3. (Color online) Blast-wave fits to STAR data [13,29–31] in semicentral Au-Au($\sqrt{s_{NN}} = 200$) collisions for transverse-momentum spectra (a) and elliptic flow (b) of ϕ, Ξ^+, and $(\Omega + \bar{\Omega})/2$ using the RL ansatz with parameters specified in Table I. Panel (c) shows the resulting Ω/ϕ ratio on a linear scale, compared with STAR data [29].

these fits (they contribute at the 10% level, which can easily be absorbed by fine-tuning the freeze-out temperature). Note that the Ω/ϕ ratio is quite different from linear for p_T up to $\sim$1.5 GeV, and that this ratio does not go to zero for $p_T \to 0$ as predicted by quark coalescence models discussed in Refs. [28,29]. This reiterates once more the importance of energy conservation and the thermal-equilibrium limit if one attempts to describe hadron spectra through quark coalescence in the low-p_T regime.

We are now in a position to extract the quark distribution functions at hadronization by assuming that (i) the flow field

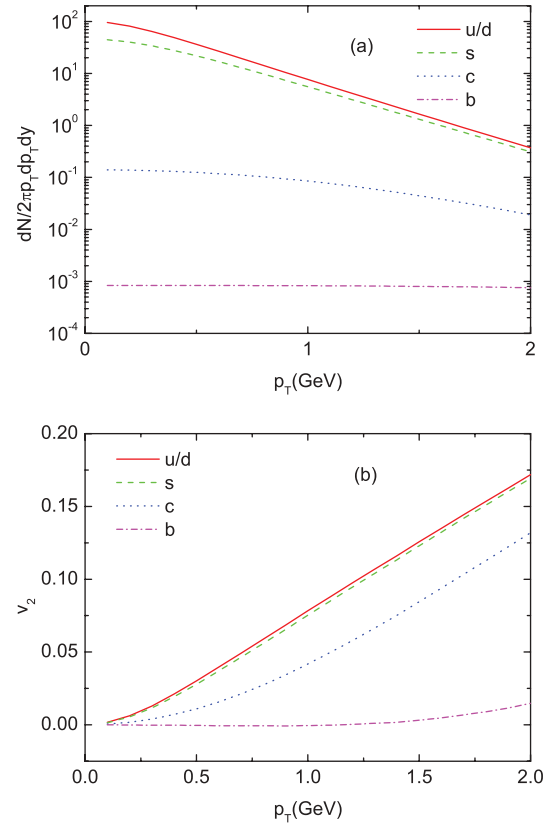

FIG. 4. (Color online) (a) Equilibrated transverse-momentum distributions of quarks on a hypersurface with temperature just above T_c for a midcentral fireball at RHIC energies as predicted by the RRM model from group-I data. (b) The same for the v_2 of the equilibrated quarks. The quark masses used (in GeV) are $m_{u/d} = 0.3$, $m_s = 0.45$, $m_c = 1.5$, and $m_b = 4.5$.

for group-I hadrons is indeed the flow field for the hadronic phase in equilibrium just below T_c (which is further supported by the fact that it is possible to use a freeze-out temperature of 180 MeV) and (ii) group-I hadron formation occurs via coalescence from a partonic phase (which is supported by the general CQNS characteristics of RHIC data). In Fig. 4, we not only include the extracted strange- and light-quark spectra and elliptic flow (which are directly involved in the RRM-based fits) but also those implied for the heavier charm and bottom quarks. Equilibration of the latter two quark flavors is currently an open issue, but this may rather be a question of how far up in p_t it applies. Qualitatively, the same limitation applies to light and strange quarks, which presumably enter the kinetic regime at $p_t \simeq 1$ GeV, where the data for the quark-number scaled v_2 level off at a value of about 7–8%. Once available, D- and B-meson data will allow for similar estimates, and we provide here the underlying heavy-quark spectra as a reference for such an analysis.

An extraction of strange- and light-quark spectra in a similar spirit, i.e., from data of what we refer to as group-I hadrons, has been attempted in Ref. [32] based on a one-dimensional instantaneous quark coalescence model. We reiterate here that such an extraction cannot be reliably applied at low p_T due to the simplifying assumptions inherent in such models, but it

would certainly be interesting to make a comparison between both approaches.

IV. BULK PARTICLES AND ROBUSTNESS OF KE$_T$ SCALING

An important aspect in the diagnosis and interpretation of universal scaling properties of the hadron-$v_2(p_T)$ is its robustness. We would like to address this question here by comparing the group-I particles with the bulk particles π, K, and p, which we refer to as group II. To do that, we first recover a fit of the RL source parametrization to the spectra and v_2 of group-II particles, as done before by the STAR Collaboration [3]. As is well known, group-II particles are characterized by the thermal freeze-out of the system at temperatures close to $T_{\rm fo} \simeq 100$ MeV, much lower than the chemical freeze-out associated with group-I particles; this is the well-known concept of sequential freeze-out. By doing so, we are essentially guaranteed to recover the universal KE$_T$ scaling as encoded in the data. However, we will then "swap" the sources for group-I and group-II particles to see how much deviation from the universal scaling is induced, which may be viewed as an upper limit. For quantitative assessment in the pion sector, the effects of feed down have to be included, which have been addressed before in coalescence models at hadronization [33,34] (where the feed-down contributions to the pion v_2 were found to be large) and at thermal freeze-out [14] (where the effects were found to be small due to small resonance abundances). Here, we evaluate the feed down at thermal freeze-out (as dictated for group-II particles which include strong resonances such as Δ and ρ), but in the presence of effective chemical potentials necessary to preserve the observed hadron ratios. As a by-product, we will obtain insight into how the source parameters evolve from chemical to thermal freeze-out (within the chosen source ansatz), which to our knowledge has not been exhibited before.

Let us recall that KE$_T$- and quark-number scaling of v_2 of group-II particles at low p_T are, by construction (thermalization at $T_{\rm fo} \simeq 100$ MeV), unrelated to quark recombination. On the one hand, n_q scaling at low p_T appears to be rather accidental. On the other hand, the mass splitting of hadrons in $v_2(p_T)$ is a signature result of ideal hydrodynamical simulations. If the hydrodynamic results are plotted versus KE$_T$, the splitting nearly vanishes, but not strictly so. In fact, a small reverse mass ordering of v_2 is found as a function of KE$_T$, as pointed out in Refs. [13,35]. In other words, the hydrodynamically induced mass splitting of $v_2(p_T)$ between light and heavy hadrons is not large enough to render their v_2(KE$_T$) curves degenerate. The sequential freeze-out picture employed here can cure this discrepancy, because the random thermal motion (which tends to isotropize p_T distributions) is suppressed at smaller temperature, which enhances the v_2 just enough to produce degeneracy in a v_2(KE$_T$) representation. The microscopic origin for the sequential hadron freeze-out is believed to be a hierarchy in the elastic cross sections: the light (bulk) hadrons π, K, and N are known to have large resonant cross sections, while no resonances are known in the scattering of the heavy multistrange hadrons on pions (or kaons). The

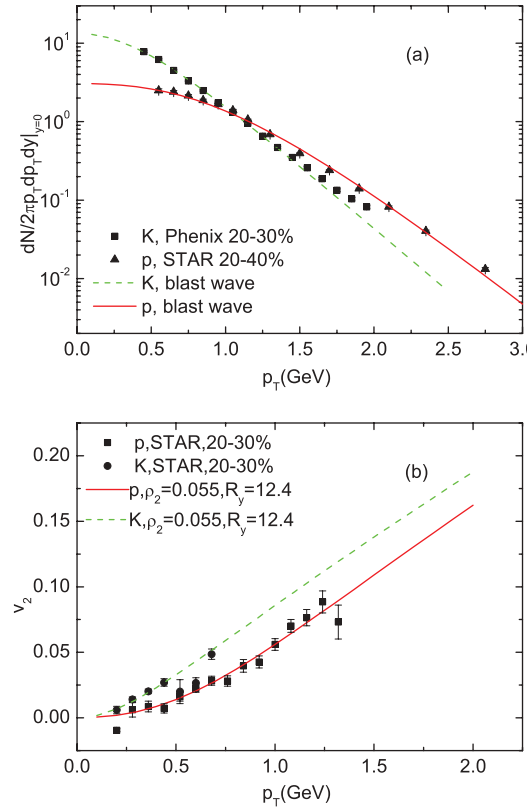

FIG. 5. (Color online) Blast-wave fits using the RL fireball parametrization to proton and kaon p_T spectra (a) and elliptic flow (b) in mid-central Au-Au collisions at RHIC. The flow-field source parameters are listed in Table I. Experimental data are taken from Refs. [3,37,38].

underlying mechanism for KE$_T$ scaling would then be general in the sense that it applies to different centralities, system sizes, and even collision energies, presumably governed by a local freeze-out criterion (with a factor of 5–10 different energy densities at chemical and thermal freeze-out [36], reflecting the difference in cross sections).

We describe group-II particle freeze-out by fitting a RL source parametrization at a typical freeze-out temperature, $T_{\rm fo} = 110$ MeV, using the p_t spectra and elliptic flow $v_2(p_T)$ of kaons and protons in semicentral Au-Au collisions (20–30% and 20–40%, respectively). The resulting spectra are shown in Fig. 5, and the corresponding parameter values for ρ_0, ρ_2, and R_y, R_x are collected in Table I (we can safely neglect chemical potentials at kinetic freeze-out since they only affect the absolute normalization of yields [36]). Pions are treated with Bose statistics which entails an appreciable (moderate) enhancement of the p_T spectra (v_2) at $p_T \lesssim 0.5$ GeV (feed-down effects are small; see below).

Let us first examine the correlation of the source parameters ρ_2 and R_y/R_x, specifically in relation to the group-I source at chemical freeze-out. As for the latter, we construct a contour in the plane of ρ_2 and R_y/R_x by varying the fits in an acceptable range given by the experimental error bars. The central value of the contours for the two groups are listed in Table I. The contour for group-II hadrons turns out to be tighter due to the larger number of (and more accurate) data

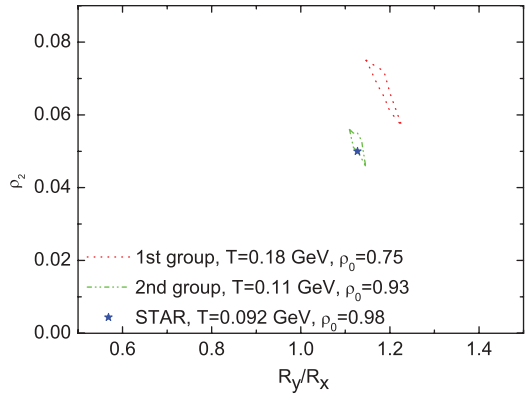

FIG. 6. (Color online) Parameter contours for ρ_2 and R_y/R_x enclosing the regions of consistency with RL blast-wave fits to p_T spectra and v_2 in the thermal regime for both freeze-out groups. The temperature T and average radial-flow rapidity ρ_0 have been fixed at $(T, \rho_0) = (180\ \text{MeV}, 0.75)$ and $(110\ \text{MeV}, 0.93)$ for groups I and II, respectively.

points for bulk particles. We have verified that using a lower freeze-out temperature of $T = 92$ MeV, as extracted by the STAR Collaboration [3], gives a ρ_2 and R_y/R_x value within our contour (star symbol in Fig. 6). The contours for the source parameters of groups I and II clearly exclude each other. This corroborates that the experimentally observed scaling of v_2 does not originate from a single freeze-out in a hydrodynamic picture.

In Fig. 7, we display the n_q-scaled hadron v_2 as a function of the n_q-scaled hadron-KE$_T$ using the values from Table I. By construction (fits to data), our calculations recover a universal scaling with deviations on the level of the experimental uncertainty (slightly larger for pions, which we discuss below). To check the stability of this result, we swap the freeze-out source for group-I and group-II particles, i.e., evaluate $v_2^{K,\pi}$ from the source at $T_c = 180$ MeV (as advocated in recombination models that neglect the hadronic phase) and the v_2^{Ω} from the source at $T_{\text{fo}} = 110$ MeV (as sometimes done in hydrodynamic calculations with a single freeze-out).

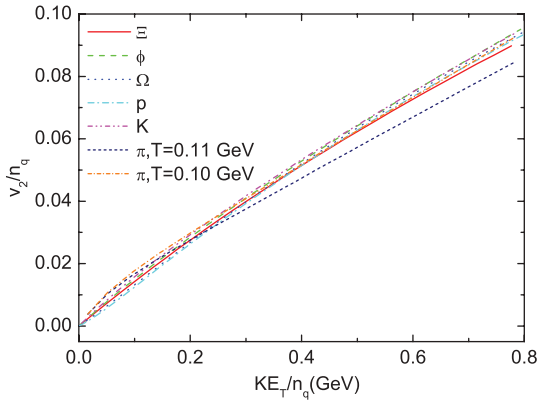

FIG. 7. (Color online) KE$_T$ and n_q scaling of v_2 for different hadrons obtained within the sequential freeze-out scenario with blast-wave parameters given in Table I. The result of a slightly later freeze-out for pions at temperature 100 MeV is also shown.

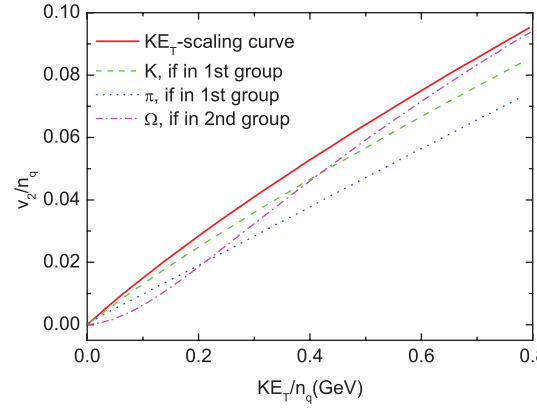

.

FIG. 8. (Color online) Comparison of the generic KE$_T$-scaling behavior of hadron-v_2 extracted from Fig. 7 (thick solid line) to results for interchanging the freeze-out configurations for group-I and group-II particles. Specifically, the Ω baryon (dash-dotted line) is frozen out from the late source at $T_{\text{fo}} = 110$ MeV, while pions (dotted line) and kaons (dashed line) are frozen out from the early source at $T_c = 180$ MeV (source parameters as quoted in Table I).

The comparison to the universal (empirical) result shows a considerable breaking of both KE$_T$ and n_q scaling that is not compatible with experimental data, but maybe not as dramatic as expected (See Fig. 8).

Let us finally return to the deviations of the pion v_2 from the scaling curve which become noticeable for KE$_T/n_q >$ 0.3 GeV in Fig. 7. First, we revisit the effects of feed-down contributions from resonances ($\rho \to \pi\pi$, $\omega \to 3\pi$, $\Delta \to N\pi$, etc.), for which conflicting statements exist in the literature [33,34]. Here we evaluate the contributions of the most important resonances decaying into pions (ρ, ω, K^*, Δ, η, K_s^0) at thermal freeze-out but with their absolute numbers correctly fixed to experiment using effective chemical potentials [36]. We find that the pion v_2 is only enhanced by a few percent over the direct pions, implying that resonance decays *do not significantly affect* the empirically found scaling. Second, we study a slight decrease of the pion freeze-out temperature from 110 MeV to, say, 100 MeV. This might be justified by a smaller thermal relaxation time of π relative to K and N, and is certainly compatible with experimental data. We find that the pion v_2 increases at higher KE$_T$, resulting in better agreement with the general scaling curve. It also reiterates the "cooling effect" of increasing the v_2 for light (bulk) particles.

V. SUMMARY AND CONCLUSIONS

In this work we have explored the consequences of hadronization of a partonic system in heavy-ion collisions via quark coalescence in local thermal equilibrium, as appropriate for low-p_T hadrons. This problem requires a recombination model which obeys four-momentum conservation and detailed balance to satisfy the correct equilibrium limit. We have reconfirmed that the resonance recombination model (RRM) complies with these properties. Specifically, we have shown

that RRM converts a quark source with a realistic flow field including nontrivial space-momentum correlations (characteristic for hydrodynamics) into hadron distributions with the same collective source properties. To our knowledge, this has not been achieved in existing models of quark coalescence. We have utilized this connection to extract quark distributions just above the critical temperature ($T_c \simeq 180$ MeV) for Au-Au collisions at RHIC from measured p_T spectra and elliptic flow of multistrange hadrons which are believed to undergo negligible final-state interactions in the hadronic phase (group-I particles).

We have furthermore verified that KE_T scaling of elliptic flow at low p_T extends to bulk particles (π, K, N = group-II particles) when a source parametrization at thermal freeze-out is employed ($T_{\mathrm{fo}} \simeq 100$ MeV). The source parameters are significantly different at T_{fo} and T_c, thus corroborating a nontrivial evolution between chemical and thermal freeze-out. In particular, we find that the scaling properties of the hadronic v_2 deteriorate if the sources for group-I and -II particles are swapped. This seems to render KE_T scaling of v_2 somewhat accidental, since for group-II particles it is not linked to quark recombination, but it does not contradict it either. It rather seems to be a consequence of the hierarchy in thermal relaxation times related to hadronic rescattering cross sections.

At intermediate p_T, the situation is expected to change, because n_q scaling seems to be a directly observable feature of quark recombination. Thus it will be an important task in future work to extend our studies with RRM to the intermediate-p_T regime where kinetic off-equilibrium effects become important. While this increases the sensitivity to quark degrees of freedom, it also requires a more detailed knowledge of the reinteractions of particles, both in the QGP and hadronic phase. Initial studies using Langevin simulations for strange and heavy quarks have been reported in Ref. [20], but the scaling properties found by the authors require a more profound understanding, including the effects of baryon formation and a more microscopic description of the elastic (as well as radiative) interactions in the QGP and hadronic matter.

ACKNOWLEDGMENTS

We gratefully acknowledge helpful discussions with H. van Hees, X. Zhao, and F. Riek. This work was supported by US National Science Foundation (NSF) Grants PHY-0449489, PHY-0847538, and PHY-0969394, by the A.-v.-Humboldt Foundation, by the RIKEN/BNL Research Center, and by DOE Grant DE-AC02-98CH10886.

[1] J. Adams *et al.* (STAR Collaboration), Nucl. Phys. A **757**, 102 (2005); K. Adcox *et al.* (PHENIX Collaboration), *ibid.* **757**, 184 (2005); I. Arsene *et al.* (BRAHMS Collaboration), *ibid.* **757**, 1 (2005); B. B. Back *et al.* (PHOBOS Collaboration), *ibid.* **757**, 28 (2005).

[2] P. Sorensen, arXiv:0905.0174v3 [nucl-ex]; S. A. Voloshin, A. M. Poskanzer, and P. Snellings, arXiv:0809.2949v2 [nucl-ex].

[3] J. Adams *et al.* (STAR Collaboration and STAR-RHIC Collaboration), Phys. Rev. C **72**, 014904 (2005).

[4] D. Teaney, J. Lauret, and E. V. Shuryak, Phys. Rev. Lett. **86**, 4783 (2001).

[5] U. Heinz, arXiv:hep-ph/0407360v1; P. F. Kolb and U. Heinz, arXiv:nucl-th/0305084v2.

[6] P. F. Kolb, J. Sollfrank, and U. Heinz, Phys. Rev. C **62**, 054909 (2000).

[7] P. Huovinen *et al.*, Phys. Lett. B **503**, 58 (2001).

[8] T. Hirano and K. Tsuda, Phys. Rev. C **66**, 054905 (2002); T. Hirano and M. Gyulassy, Nucl. Phys. A **769**, 71 (2006).

[9] S. A. Voloshin, Nucl. Phys. A **715**, 379c (2003).

[10] D. Molnar and S. A. Voloshin, Phys. Rev. Lett. **91**, 092301 (2003); R. J. Fries, B. Muller, C. Nonaka, and S. A. Bass, Phys. Rev. C **68**, 044902 (2003); V. Greco, C. M. Ko, and P. Levai, *ibid.* **68**, 034904 (2003); R. Fries, V. Greco, and P. Sorensen, Annu. Rev. Nucl. Sci. **58**, 177 (2008).

[11] S. Pratt and S. Pal, Nucl. Phys. A **749**, 268 (2005); D. Molnar, arXiv:nucl-th/0408044v2; V. Greco and C. M. Ko, arXiv:nucl-th/0505061v2.

[12] A. Adare *et al.* (PHENIX Collaboration), Phys. Rev. Lett. **98**, 162301 (2007); B. I. Abelev *et al.* (STAR Collaboration), Phys. Rev. C **75**, 054906 (2007).

[13] B. I. Abelev *et al.* (STAR Collaboration), Phys. Rev. C **77**, 054901 (2008).

[14] L. A. Linden Levy, J. L. Nagle, C. Rosen, and P. Steinberg, Phys. Rev. C **78**, 044905 (2008).

[15] R. A. Lacy and A. Taranenko, arXiv:nucl-ex/0610029v3.

[16] J. Tian *et al.*, Phys. Rev. C **79**, 067901 (2009).

[17] J. Jia and C. Zhang, Phys. Rev. C **75**, 031901(R) (2007).

[18] L. Ravagli and R. Rapp, Phys. Lett. B **655**, 126 (2007).

[19] W. Cassing and E. L. Bratkovskaya, Phys. Rev. C **78**, 034919 (2008).

[20] L. Ravagli, H. van Hees, and R. Rapp, Phys. Rev. C **79**, 064902 (2009).

[21] H. van Hees, V. Greco, and R. Rapp, Phys. Rev. C **73**, 034913 (2006).

[22] O. Barannikova (STAR Collaboration), arXiv:nucl-ex/0403014.

[23] B. Mohanty and N. Xu, J. Phys. G **36**, 064022 (2009).

[24] R. J. Fries, R. J. Muller, C. Nonaka, and S. A. Bass, Phys. Rev. Lett. **90**, 202303 (2003); V. Greco, C. M. Ko, and P. Levai, *ibid.* **90**, 202302 (2003); R. C. Hwa and C. B. Yang, Phys. Rev. C **67**, 034902 (2003).

[25] F. Retiere and M. A. Lisa, Phys. Rev. C **70**, 044907 (2004).

[26] J. D. Bjorken, Phys. Rev. D **27**, 140 (1983); R. C. Hwa, *ibid.* **10**, 2260 (1974).

[27] E. Schnedermann, J. Sollfrank, and U. Heinz, Phys. Rev. C **48**, 2462 (1993).

[28] R. C. Hwa and C. B. Yang, Phys. Rev. C **75**, 054904 (2007).

[29] B. I. Abelev *et al.* (STAR Collaboration), Phys. Rev. Lett. **99**, 112301 (2007).

[30] J. Adams *et al.* (STAR Collaboration), Phys. Rev. Lett. **98**, 062301 (2007).

[31] B. I. Abelev *et al.* (STAR Collaboration), Phys. Rev. C **79**, 064903 (2009).
[32] H. Z. Huang, J. Phys. G **36**, 064008 (2009); J. H. Chen, F. Jin, D. Gangadharan, X. Z. Cai, H. Z. Huang, and Y. G. Ma, Phys. Rev. C **78**, 034907 (2008).
[33] V. Greco and C. M. Ko, Phys. Rev. C **70**, 024901 (2004).
[34] X. Dong *et al.*, Phys. Lett. B **597**, 328 (2004).
[35] U. Heinz, arXiv:0901.4355 [nucl-th].
[36] R. Rapp, Phys. Rev. C **66**, 017901 (2002).
[37] B. I. Abelev *et al.* (STAR Collaboration), Phys. Rev. Lett. **97**, 152301 (2006).
[38] S. S. Adler *et al.* (PHENIX Collaboration), Phys. Rev. C **69**, 034909 (2004).